Carnegie Mellon University

Prediction of laser absorptivity from synchrotron x-ray images using deep convolutional neural networks

Runbo Jiang[a], Joseph Aroh[a], Brian Simonds[b], Tao Sun[c], Anthony D. Rollett[a]

[a] Department of Materials Science and Engineering, Carnegie Mellon University

[b] Applied Physics Division, National Institute of Standards and Technology

[c] Department of Materials Science and Engineering, University of Virginia

Oct, 2022

Table of Contents

It is critical to measure the laser absorption

- The absorbed laser light is the dominant energy source that induces vapor cavity formation during laser melting process in additive manufacturing
- Direct measurement
    - collection of reflected light via an integrating sphere which are difficult and expensive
- Modeling methods
    - Empirical absorptivity model for **conduction mode** melt pools based on the width of melt pool using Rosenthal equation

$$\eta_{pre} = \frac{\pi k(T_m - T_0)W + 0.125 e\pi\rho C(T_m - T_0)VW^2}{P}$$

    - High-fidelity multiphysics model use a laser ray-tracing method to interpret energy absorption

$$\eta = \eta_{\mathrm{absor}} = 0.7\left[1 - \exp(-0.6\mathrm{Ke_m}L_d^*)\right], \quad (6)$$

$$\mathrm{Ke_m}L_d^* = \frac{\eta_m P}{(T_l - T_0)\pi\rho C_p\sqrt{\alpha V_s r_0^3}} \cdot \sqrt{\frac{\alpha}{V_s r_0}} = \frac{\eta_m P}{(T_l - T_0)\pi\rho C_p V_s r_0^2}. \quad (7)$$

Gan, Z., et al. (2020). Universal scaling laws of keyhole stability and porosity in 3D printing of Metals.

Causal relationship between melt pool geometry and absorption

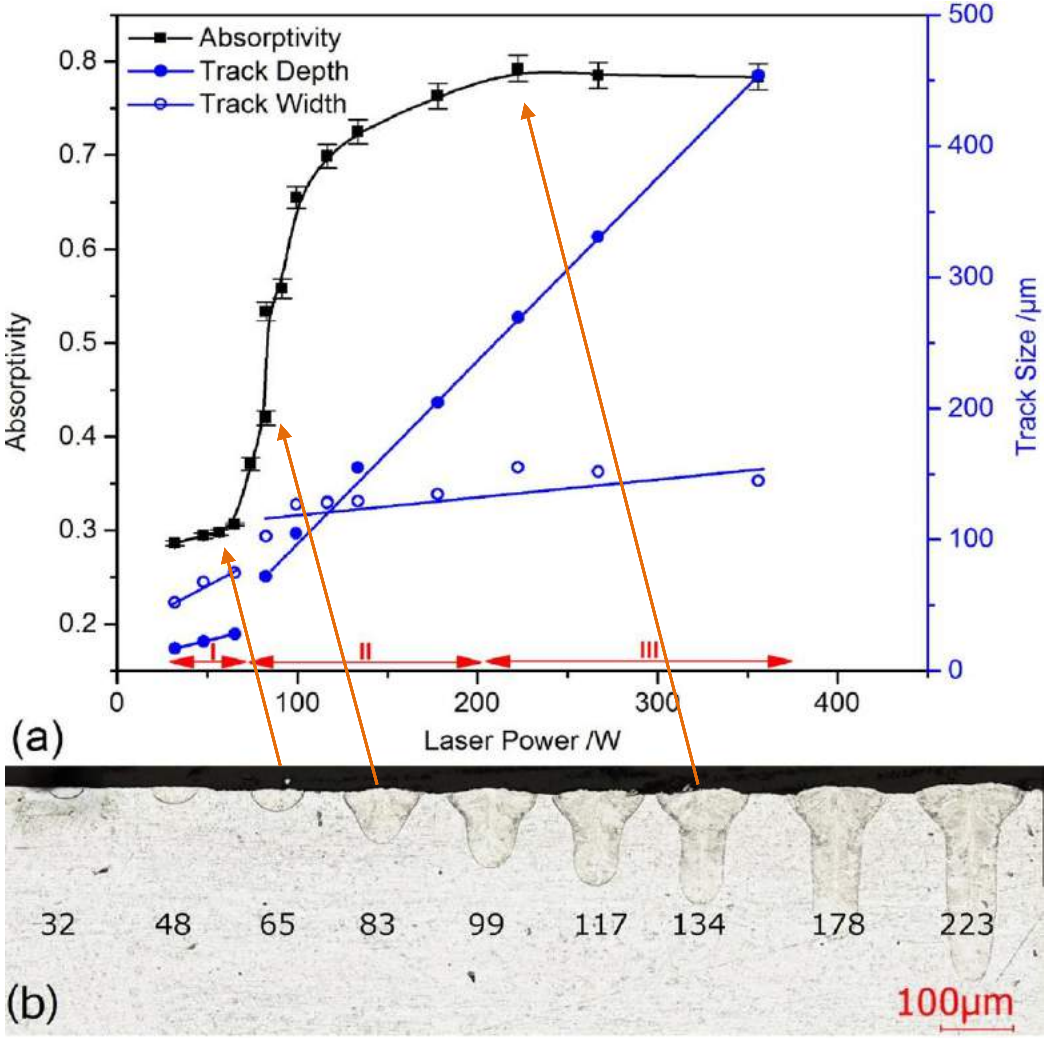

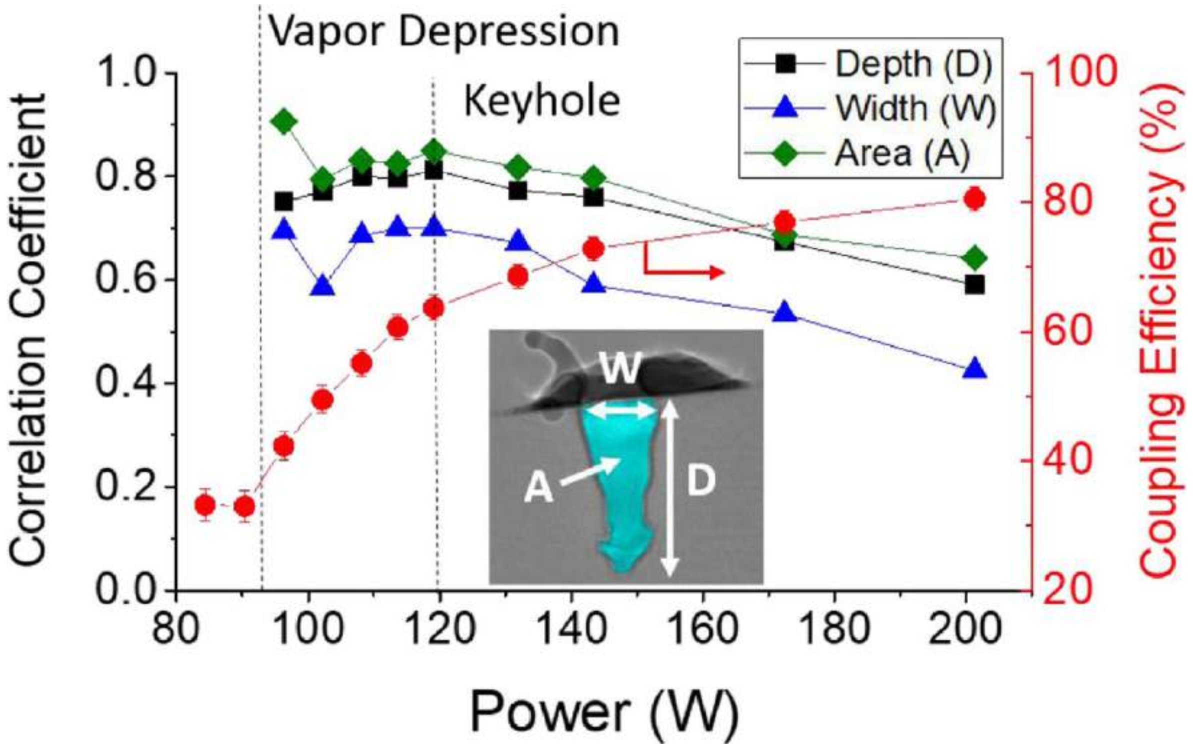

The Spearman correlation coefficient for cavity depth, area, and width (defined in inset) versus laser power for stationary laser melting of a bare Ti-6Al-4V plate.

Simonds, B., et al. (2021). The causal relationship between melt pool geometry and energy absorption measured in real time during laser-based manufacturing. *Applied Materials Today*, *23*, 101049.

Trapp, J., et al. (2017). In situ absorptivity measurements of metallic powders during laser powder-bed fusion additive manufacturing. *Applied Materials Today*, *9*, 341–349.

In situ laser absorptivity measurement

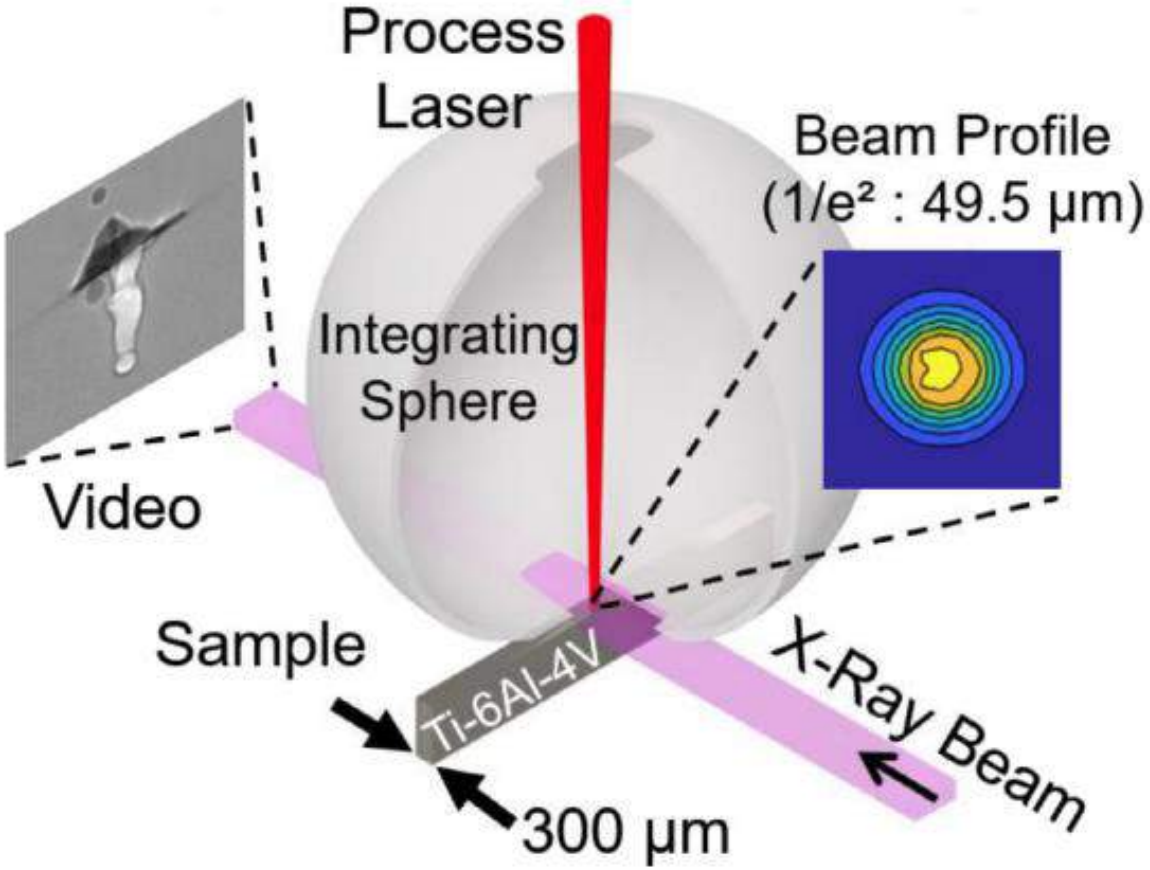

Schematic of the high-speed synchrotron imaging and laser absorption setup at APS Advanced Photon Source.

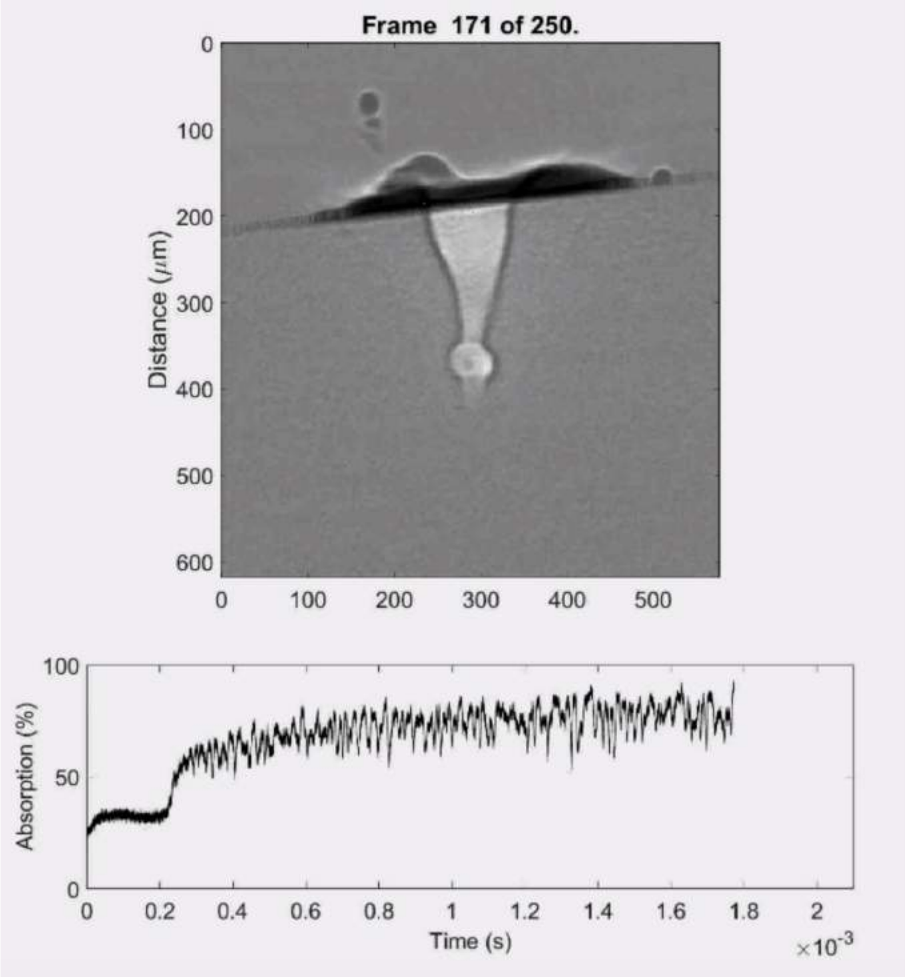

A synchrotron image cross-section of the melting pool and dynamic laser absorption.

Simonds, B., et al. (2021). The causal relationship between melt pool geometry and energy absorption measured in real time during laser-based manufacturing. *Applied Materials Today*, 23, 101049.

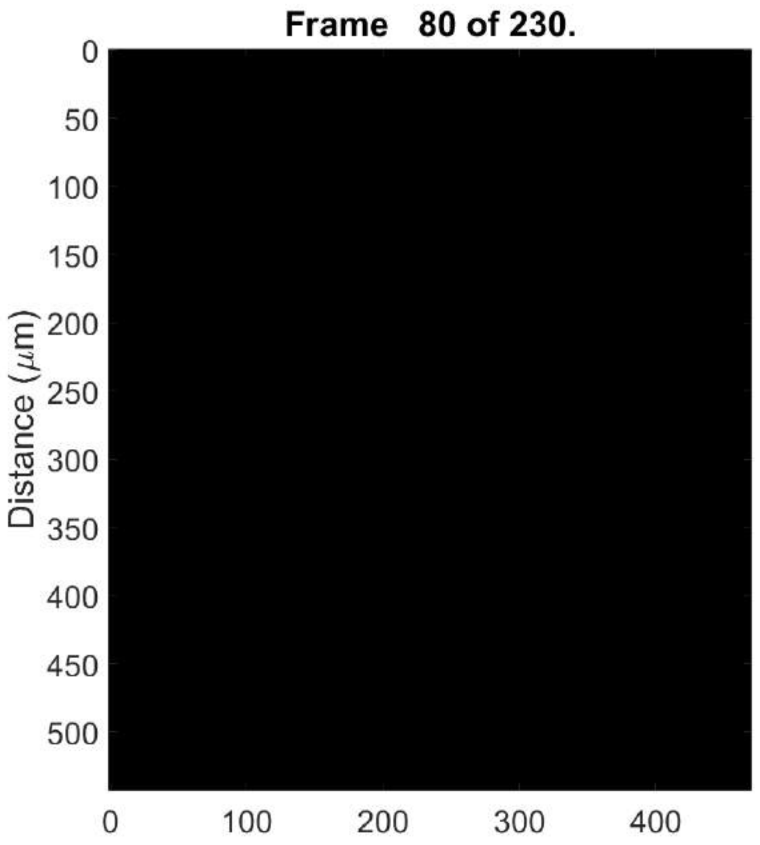

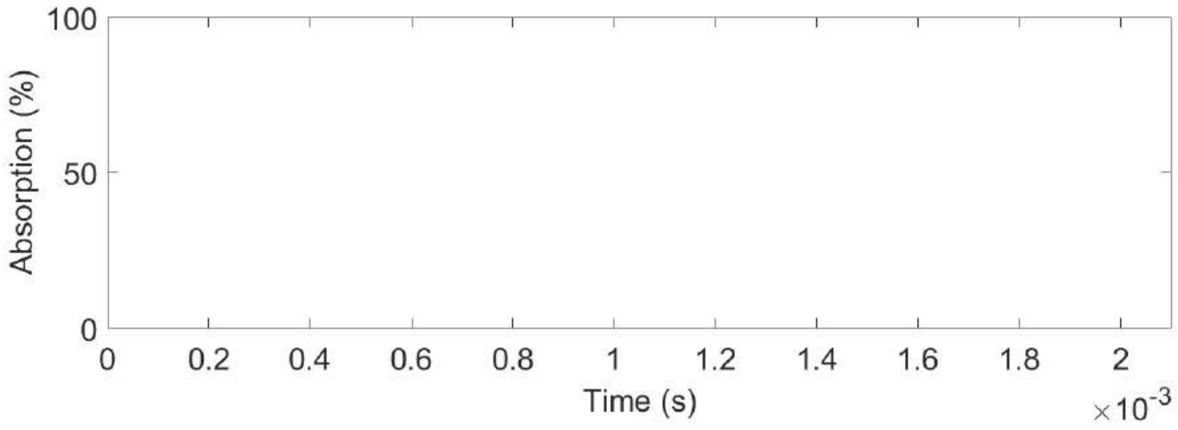

Simonds, B., et al. (2021). The causal relationship between melt pool geometry and energy absorption measured in real time during laser-based manufacturing. *Applied Materials Today, 23*, 101049.

Dataset

- Training and validation datasets consist spot welding Ti64 data from 4 laser powers: **119W, 125W, 151W, and 189W**
- In total, we have 926 images, and we split the data 80% for training 20% for validation
- For test dataset, we hold out another entire spot weld data of 226 frames

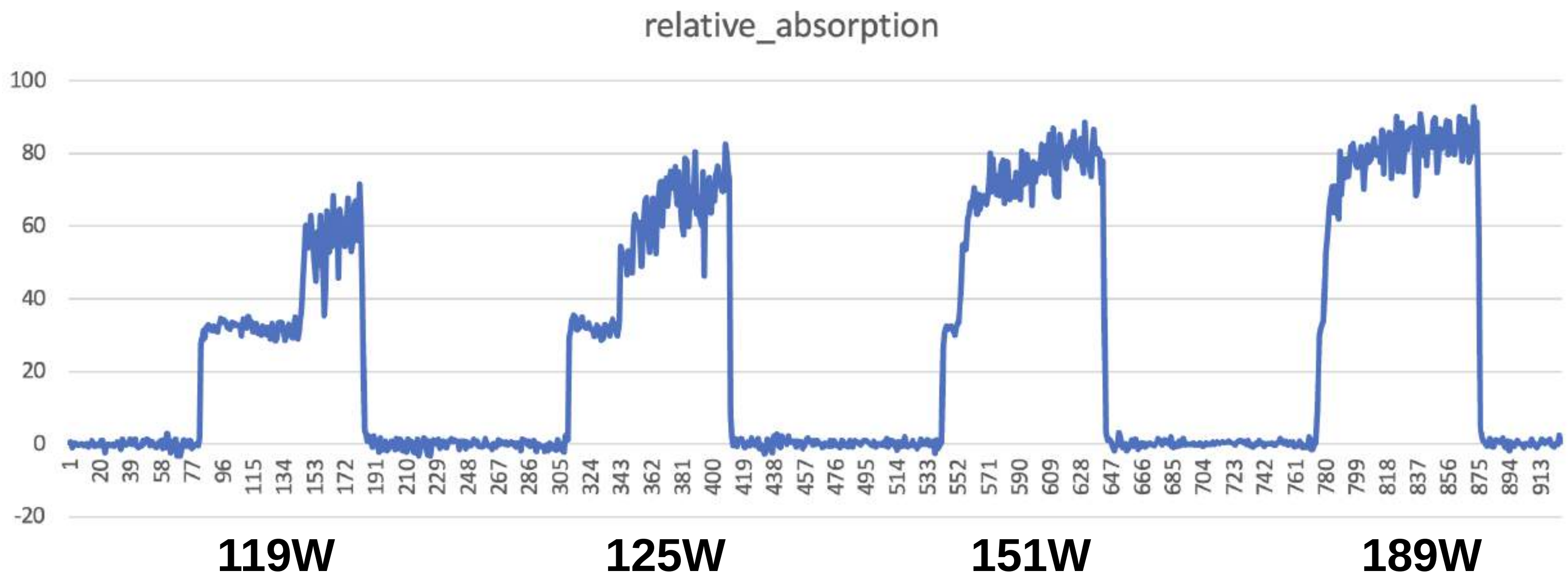

Data preprocessing and augmentation

- Divide each frame by the first frame to remove background noise, then normalize to [0,255]
- First cropped into size 300 x 300 pixels with the vapor cavity roughly in the center of each image
- To feed images into pretrained models, images are first resized into 256 x 256, then center cropped into 224 x 224
- To improve model's generalizability, data augmentation is essential in deep learning tasks
    - Random rotation by 7 degree
    - Random horizontal flip

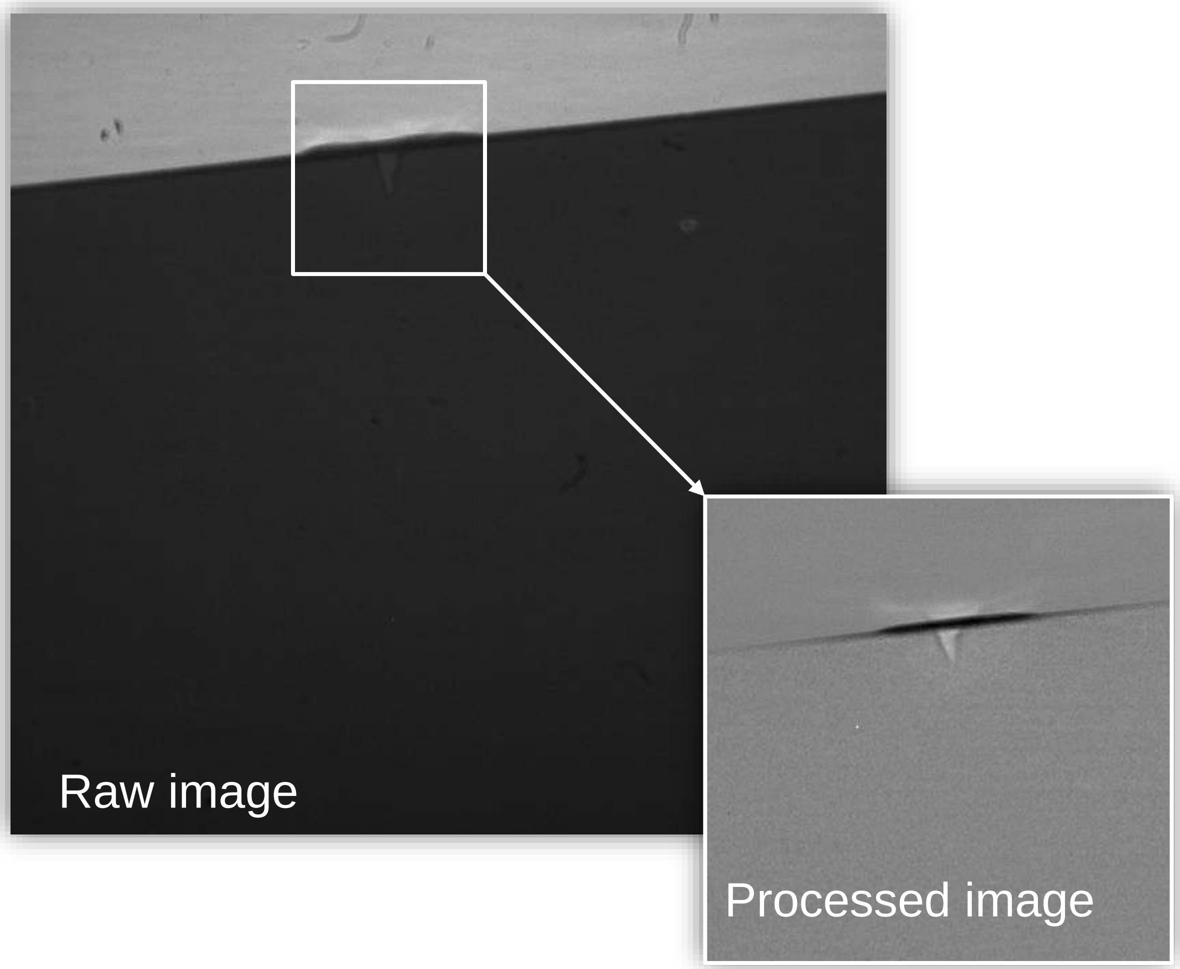

ConvNet Models

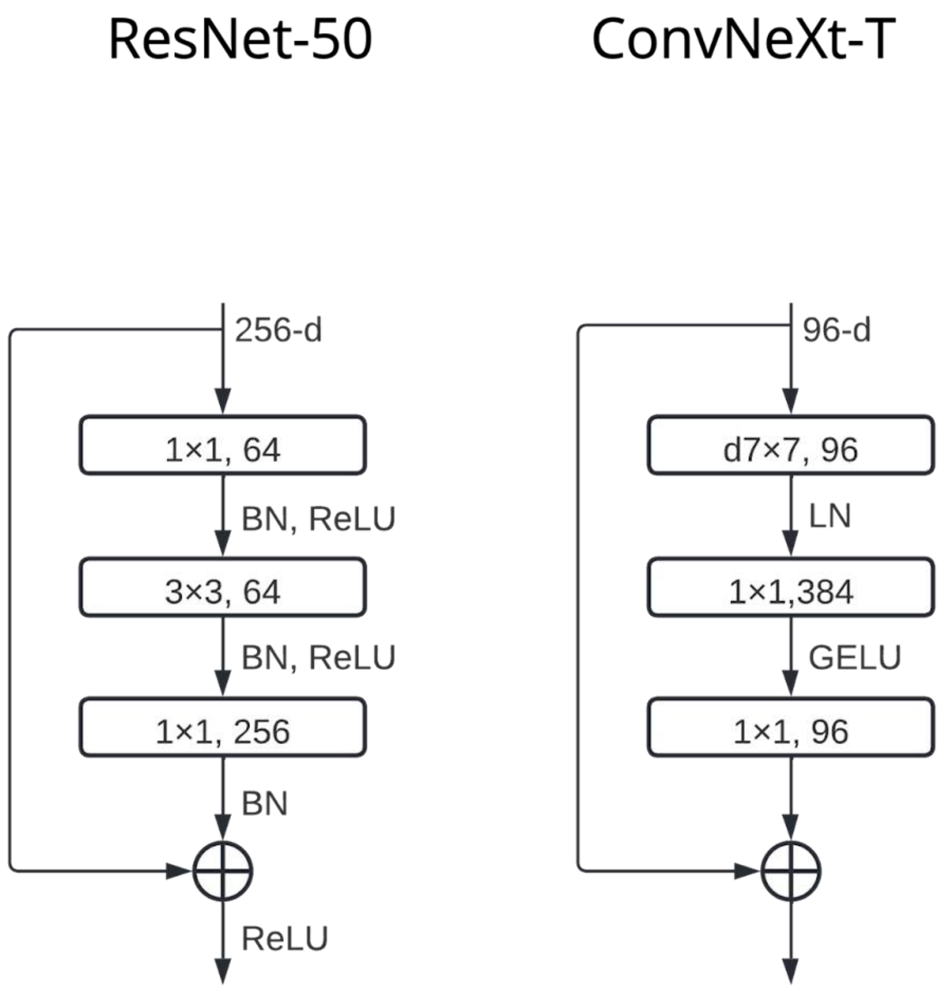

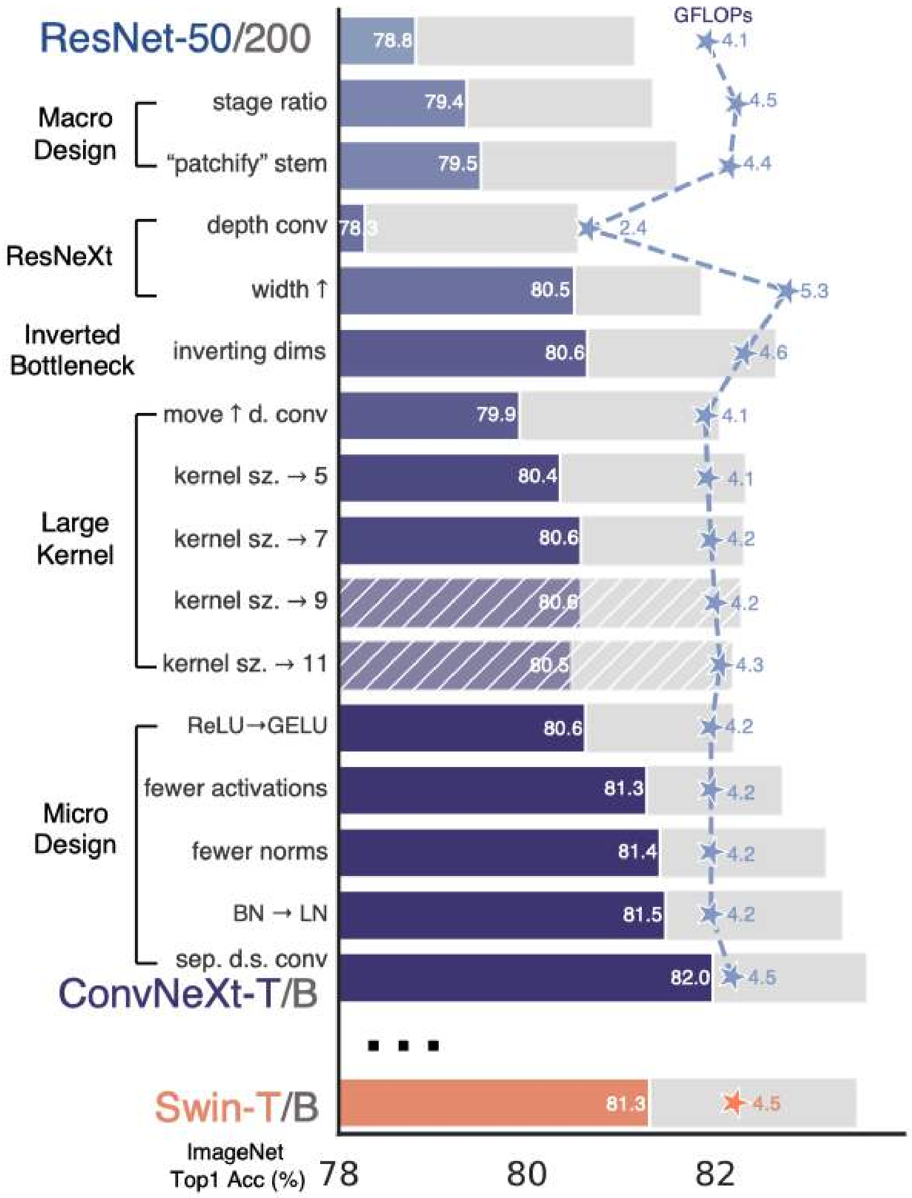

A ConvNet for the 2020s. Liu et al. 2022

Model training setup using in-domain dataset

Modifications made for this regression task:

- Stack each x-ray images 3 times to simulate an RGB images
- Output size of fully connected layer
- Loss function MAE

Training setup

model	#parameters	batch size	initial lr	optimizer	weight decay
Resnet50	23,510,081	128	1e-3	AdamW	0.05
ConvNext_tiny	27,814,273	16	3e-5	AdamW	0.05

Training and validation loss

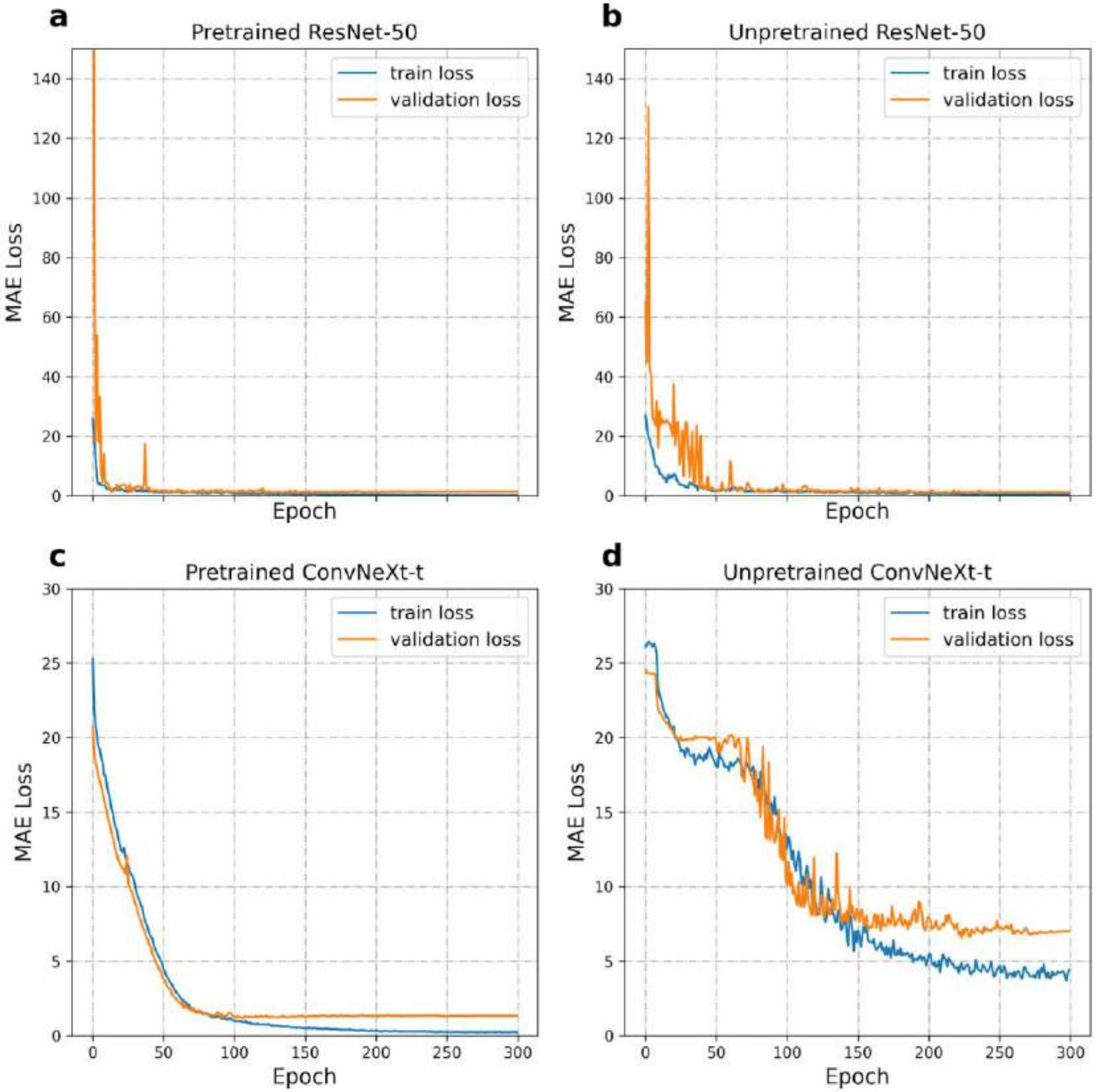

Model	if pretrained	train loss	val loss	test loss
ResNet50	pretrained=True	0.2139	1.4044	4.5335
	pretrained=False	0.4583	1.2890	8.1304
ConvNeXt	pretrained=True	0.2129	1.3232	5.9008
	pretrained=False	4.4071	6.9980	22.0075

- Both pretrained resnet-50 and ConvNext-t are pertained on the 1000-class ImageNet classification dataset
- Loss curves are decreasing more smoothly in both pretrained models, which also eventually lead to a lower loss -> good transferability to unrelated dataset

Model performance on test data

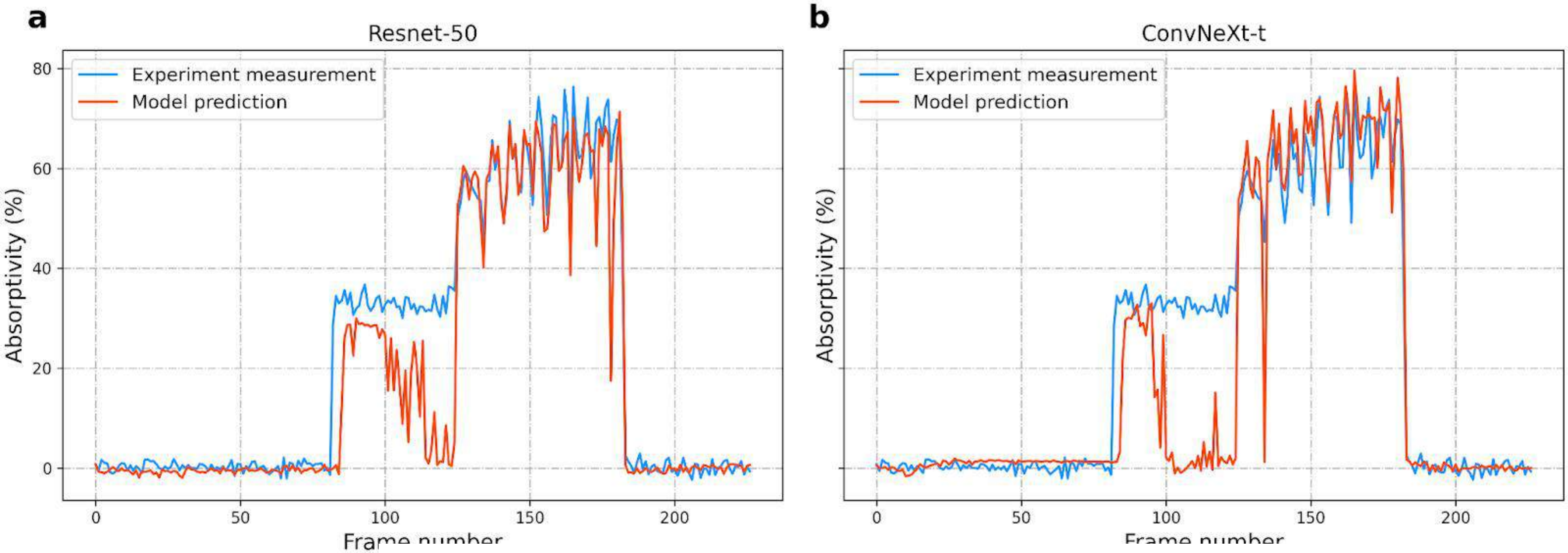

- Prediction error
  features a high l … vity
- Error is significa … ata

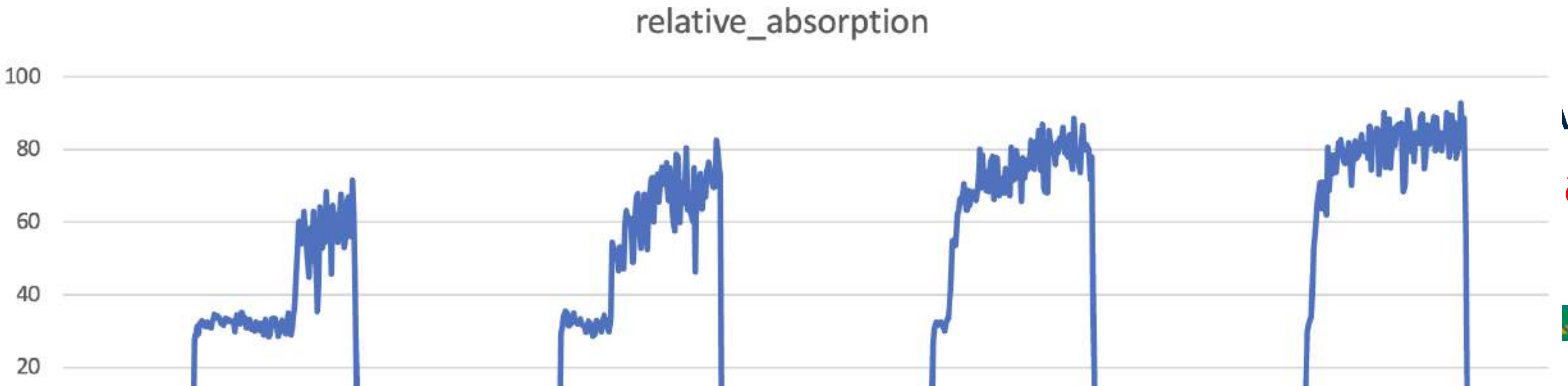

Feature Maps

Visualize what the c e image.

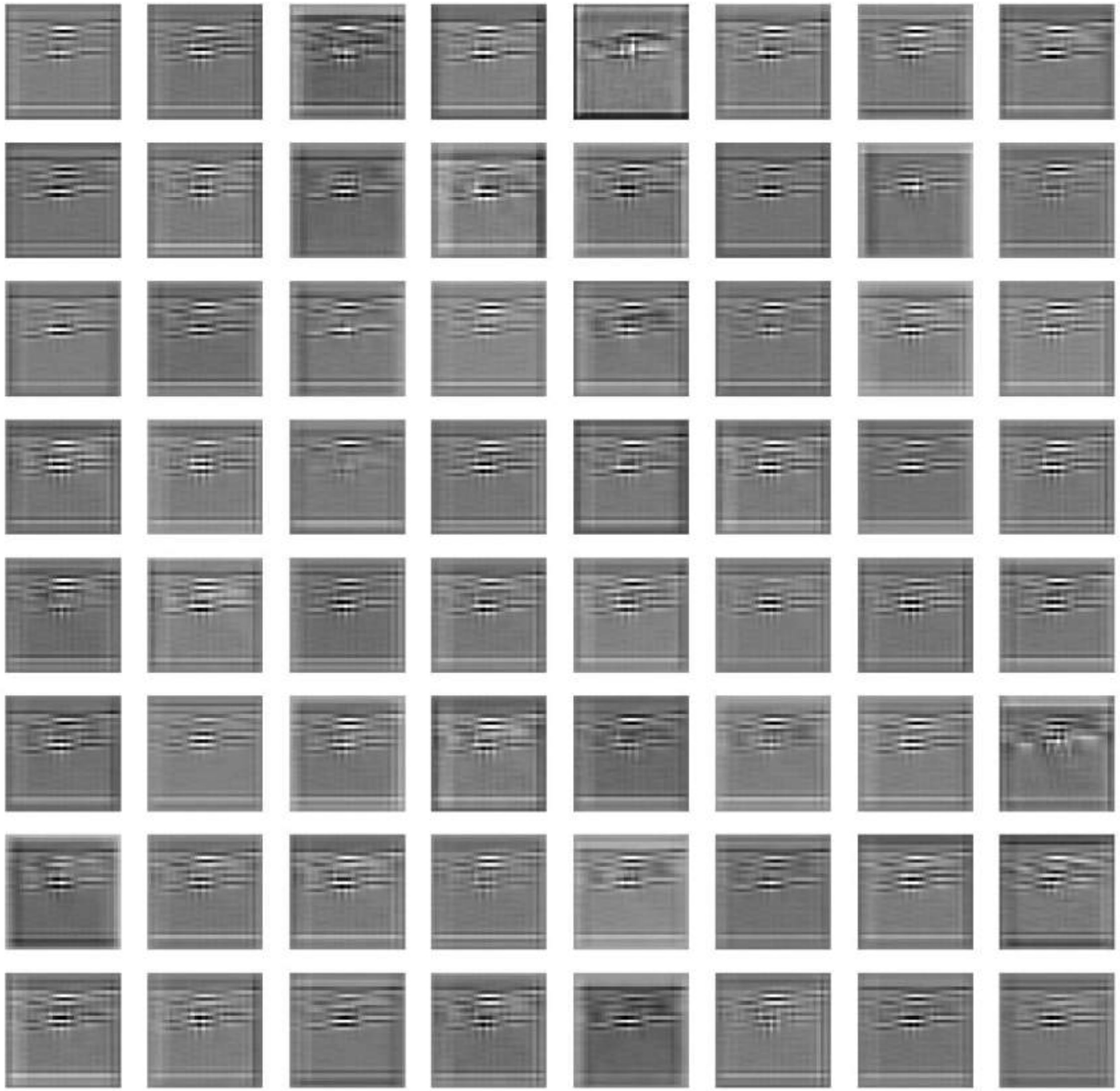

CAM for visualizing where deep learning networks pay attention

Class activation maps (CAM) are a simple technique to get the discriminative image regions used by a ConvNet to identify a specific class in the image. In other words, a class activation map (CAM) lets us see which regions in the image were relevant to this class.

Resnet

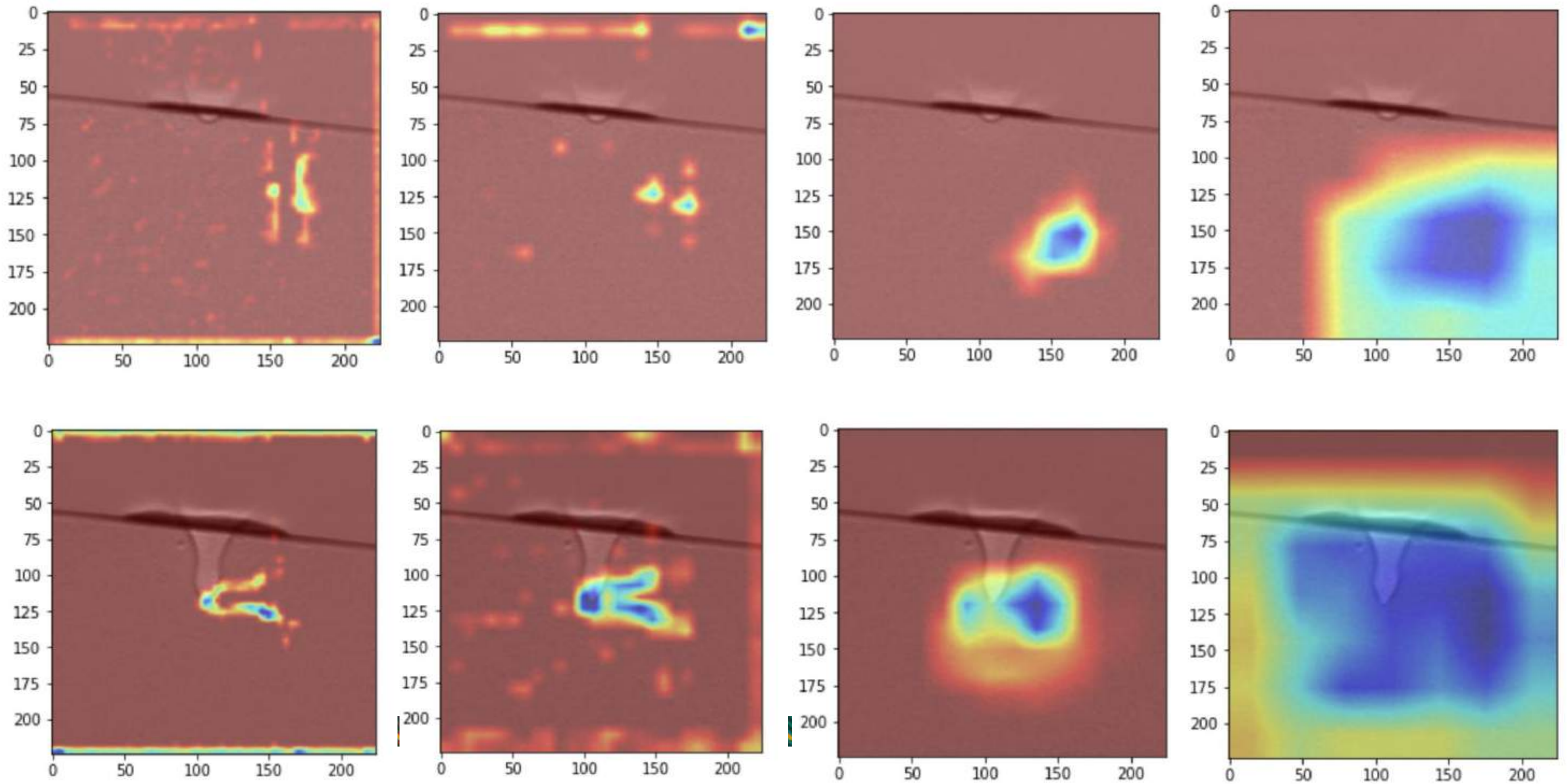

Future Work:

Two stage absorptivity prediction

Motivation

- better understanding of the correlation between features and absorptivity
- Robust and accurate image segmentation

Current keyhole segmentation pipeline uses OpenCV package

Limitations

- Requires manual parameter tunning at multiple steps
- Accurate performance on deep keyholes but struggles to differentiate shallow keyholes with background noise
  - Shallow keyhole tends to be considered as background noise
  - At the end the code pick up the largest object as the keyhole

Pyeon, J ., et al. (2021). Time-Resolved Geometric Feature Tracking Elucidates Laser-Induced Keyhole Dynamics. IMMI, 10:677–688.

Semantic image segmentation using deep learning methods

- Image Segmentation Models
  - U net + Resnet/MobileNet/ConvNext
  - Deeplab +Resnet/MobileNet /ConvNext
- Regression Models
  - LR/Boosting/Bagging models
- Dataset:
  - Both moving laser and stationary laser images
  - Balance the amount of samples with deep keyhole and **shallow keyhole**

Table 2 The performance (IoU) of all six semantic segmentation models

Semantic segmentation models	Intersection over Union (IoU)
FCN (Model i)	0.785 ± 0.127
U net (Model ii)	0.628 ± 0.102
U net + MobileNet (Model iii)	0.929 ± 0.003
U net + ResNet50 (Model iv)	0.902 ± 0.013
Deeplab v3 (Model v)	0.93 ± 0.008
Deeplab + MobileNet (Model vi)	0.936 ± 0.01

Zhang, J ., et al. (2022). Image segmentation for defect analysis in laser powder bed fusion: Deep data mining of X-ray photography from recent literature. IMMI, *11*(3), 418–432.

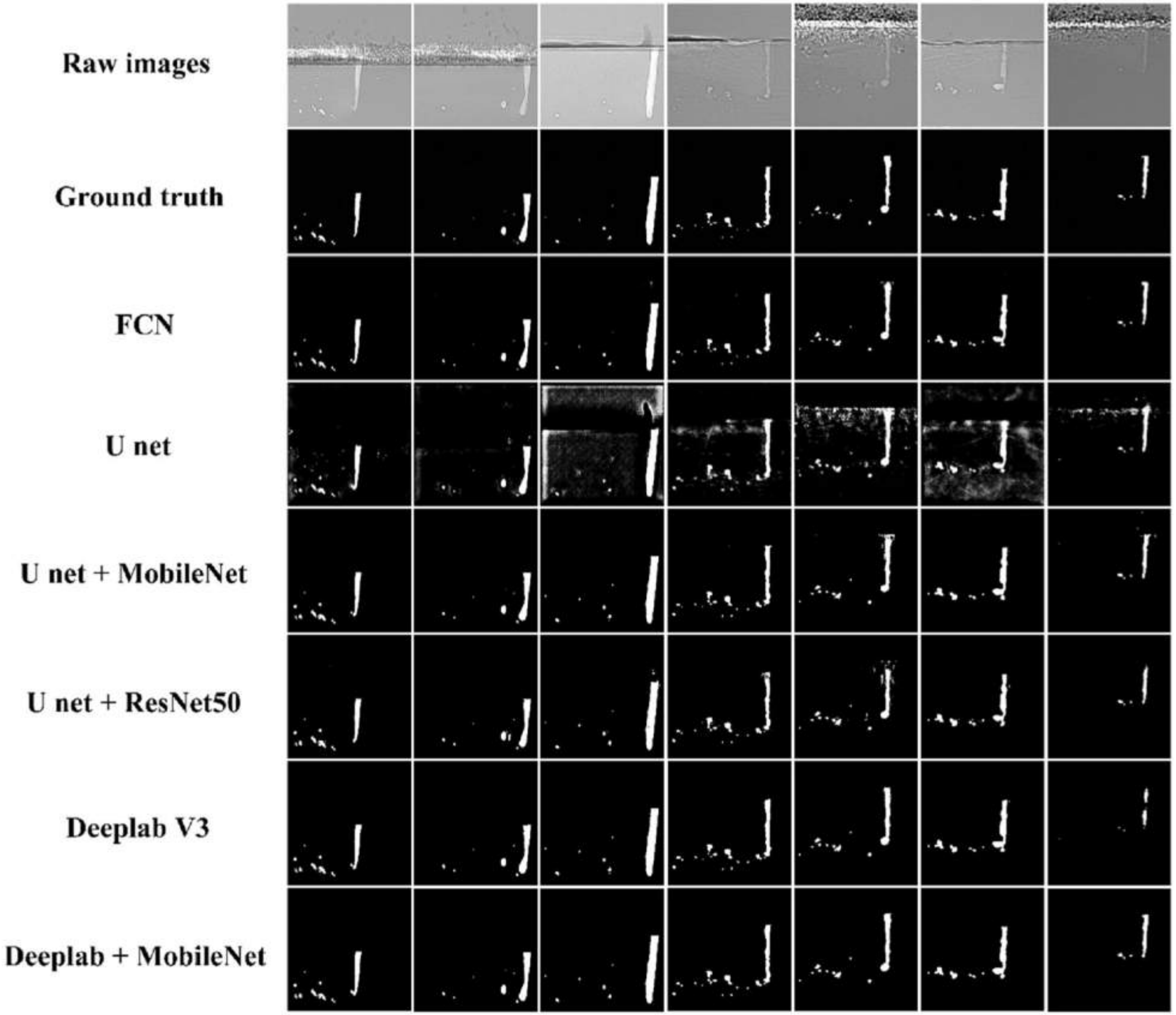

Illustration of the semantic segmentation results on the X-ray : from movies S1-S7 [12, 13]. The first two rows are the raw image and the ground truth. The remaining rows show the predicted results from the six semantic segmentation models. The U net + MobileNet model and the Deeplab + MobileNet model perform best, whereas the U net mode predicts least accurately among all

Table 1 X-ray images obtained from the melting processes of Ti64 and Al7A77 under various processing parameters [12, 13]

Movies	Material	Power (W)	Scan speed (mm/s)	With or without powder	Number of images
S1	Ti–6Al–4V	382	500	Y	126
S2	Ti–6Al–4V	382	525	Y	116
S3	Ti–6Al–4V	382	475	N	126
S4	Al7A77	500	600	N	81
S5	Al7A77	500	600	Y	78
S6	Al7A77	500	800	N	57
S7	Al7A77	500	1000	Y	44

Zhang, J ., et al. (2022). Image segmentation for defect analysis in laser powder bed fusion: Deep data mining of X-ray photography from recent literature. IMMI, *11*(3), 410–420.

Summary

- Developed a pipeline to predict laser absorptivity for Ti64 given spot welding keyhole images
- Pretrained ConvNet models achieves lower MAE on the in-domain keyhole dataset
- Proposed a two-stage pipeline that involves a robust image segment process and a regression task

Acknowledgement

- Brian Simonds at NIST for sharing the data
- Katelyn Jones for ConvNet discussion

Thank you!
Any questions?

Runbo Jiang
runboj@andrew.cmu.edu